Applied Surface Science 351 (2015) 746–752

Contents lists available at ScienceDirect

Applied Surface Science

journal homepage: www.elsevier.com/locate/apsusc

Exploring the effect of boron and tantalum codoping on the enhanced photocatalytic activity of TiO_2

Yinyan Gong*, Chengxin Fu, Lv Ting, Jingru Chenu, Qinger Zhao, Can Li

Center for Coordination Bond Engineering, School of Materials Science and Engineering, China Jiliang University, Hangzhou 310018, Zhejiang, China

ARTICLE INFO

Article history:
Received 2 March 2015
Received in revised form 25 May 2015
Accepted 31 May 2015
Available online 6 June 2015

Keywords:
Codoping
Boron
Tantalum
TiO_2 nanocrystals
Photocatalysts

ABSTRACT

Aiming to improve the photocatalytic activity, boron and tantalum co-doped TiO_2 nanocrystals were prepared by a sol–gel method. Pure and doped titania samples were characterized by X-ray diffraction (XRD) measurements, Raman spectroscopy, X-ray photoelectron spectroscopy (XPS) and UV–vis diffuse reflectance spectroscopy. The results revealed that all the samples have highly crystalline anatase structure, and no any other second phase was observed. It is found that the incorporation of dopants inhibits the growth of TiO_2 nanocrystal. Moreover, XPS observations showed that Ta are in the form of Ta^{5+} while the majority of B species are present at interstitial sites. Finally, photocatalytic activities of all the samples were evaluated by degradation of methylene blue (MB) solutions under simulated solar light irradiation. Ta-doped and (B, Ta)-codoped catalysts exhibit enhanced photocatalytic activities in comparison with pure TiO_2, with the codoped sample exhibiting the best photodegradation performance. This indicates that B and Ta co-doping is an effective way to improve photocatalytic performance of TiO_2. The catalytic activity of B-doped TiO_2 becomes slightly worse than pure TiO_2 nanocrystals, which is plausible due to increased charge carrier recombination centers induced by incorporation of boron species.

1. Introduction

Titania (TiO_2) has drawn great interests as a promising photocatalyst for hydrogen fuel production, and water and air purification because of its natural abundance, chemical stability, non-toxicity, and low cost [1–4]. However, the large-scale applications of TiO_2 are hindered by its low efficiency under sunlight irradiation. This is mostly attributed to the fast recombination of electron–hole pairs and a relatively large energy gap of TiO_2 (E_g = 3.2 eV for anatase phase and E_g = 3.0 eV for rutile phase), limiting its light absorption to the ultraviolet fraction of the solar energy spectrum [1,2,5]. Numerous efforts have been devoted to extending the optical response regime of TiO_2 toward visible region, and/or suppress the charge carrier recombination [1,2,6–15].

One frequently used method involves the incorporation of nonmetal [6,7,16–19], or metal dopants [8,20–23]. However, mondoping has inadvertently increased recombination losses, and thus did not always lead to significant improvement of photocatalytic activities companying the extension of photo-response region [10,24,25]. Several factors might contribute to the observed limited photocatalytic activity of mondoped TiO_2. For example, it has been reported previously that N-doping creates localized midgap states, and at the meantime favors the formation of oxygen vacancies (CBM) [25,26], which might also act as recombination centers for photo-excited charge carriers. Another example is that although the band gap of TiO_2 can be reduced by doping with 3d metal ions, the carrier mobility will be reduced due to the existence of recombination centers as well as the formation of the strongly localized d states within the band gap [27,28].

Recently, codoping has been proposed as a promising approach to address the conflicting issue of visible light absorption enhancement and charge carrier recombination in singly doped TiO_2. Specifically, both non-metal and metal species are incorporated spontaneously into TiO_2 to suppress the formation of charge carrier recombination centers and increase the solubility limits of dopants, which is typically low in wide band gap semiconductors [24,29–36]. For example, Jaiswal et al. [29], reported that (N, V)-codoped titania demonstrates better visible photocatalytic activity for degradation of Rhodamine B than singly doped samples. Bloh et al. [30], studied the physicochemical properties and band structure of (N, W)-codoped TiO_2, and suggested that N doping can extend the absorption edge toward visible region while the co-existence of W facilitate the incorporation and stabilization of N. Moreover, Lim et al. [31], observed superior photocatalytic activity of (N, Nb)-codoped TiO_2 to N and Nb singly doped samples. They suggested that codoping of N and Nb can effectively maintain charge

* Corresponding author.
E-mail addresses: ygong2007@163.com, ygong2007@gmail.com (Y. Gong).

http://dx.doi.org/10.1016/j.apsusc.2015.05.187
0169-4332/

neutralization and stabilize the crystal structure. In addition, Hoang et al. [32], investigated the photoelectrochemical performance of (N, Ta)-codoped TiO_2 nanowires, and attributed the enhancement to the fewer recombination centers in the co-doped samples. Up to now, the most commonly used anion dopant involved in codoping is nitrogen, whereas there are very limited studies on codoping metal species with B. It has been reported previous that (B, La)-codoped [33] and (B, Ni) [34] and TiO_2 can effectively improve the photocatalytic activity of TiO_2. Recently, Deng's group reported that (B, Ag)-codoping leads to high photocatalytic activity of TiO_2 under simulated solar-light irradiation, and proposed that tricoordinated interstitial boron [B_{int}] species and Ag ions form [B_{int}–O–Ag] structure units, which act as shallow trap for electrons and prolong lifetime of the photoinduced charge carriers [37].

In this work, we are mainly focused on exploring the effect of B and Ta codoping on the photocatalytic activity of TiO_2. Pure, B-doped, Ta-doped, and (B, Ta)-codoped TiO_2 nanocrystals were prepared by a sol–gel method. Photocatalytic activity was evaluated by degradation of aqueous methylene blue (MB) solution under simulated solar light irradiation. The co-doped sample has the highest degradation efficiency, which is about twice that of pure TiO_2, indicating that co-doping TiO_2 with B and Ta is an effective approach to improve photocatalytic performance. Various characterization techniques including powder X-ray diffraction measurements (XRD), Raman spectroscopy, X-ray photoelectron spectroscopy (XPS), EDX spectroscopy, and UV–vis diffuse reflectance spectroscopy measurements were performed to investigate the effect of B and Ta doping on the structural, electronic and optical properties of TiO_2.

2. Experimental

2.1. Material synthesis

All chemicals were commercially available and used as received without further purification or pre-treatment. They include titanium butoxide (98.0%, Aladdin), acetic acid (99.5%, Hangzhou Gaojing), boric acid (99.5%, Aladdin), ethanol (99.7%, Hangzhou Gaojing), and tantalum pentachloride (99.8%, Aldrich).

Pure, Ta-doped, B-doped, and (B, Ta)-codoped TiO_2 nanocrystals were prepared using a sol–gel method. Initially, a titanium precursor solution was prepared by mixing 17 ml titanium butoxide with 30 ml ethanol under constant stirring at room temperature for 30 min, referred to as solution A. Independently, solution B was prepared by mixing 28 ml ethanol, 10 ml acetic acid, and 3 ml DI water. To prepare (B, Ta)-codoped TiO_2, 0.0927 g H_3BO_3 and 0.5373 g $TaCl_5$ (with the nominal molar ratios of B/Ti = Ta/Ti = 0.03) were dissolved in solution B, which was added dropwise to solution A under vigorous stirring. The resultant translucent mixture was stirred for 4 hrs at room temperature, followed by aging for 24 h, and then dried in oven at 80 °C for 12 h. Finally, the obtained dry gels were grounded and calcined in a muffle furnace at 500 °C for 3 h to obtain TiO_2 powder. A similar method was employed to prepare pure (B/Ti = Ta/Ti = 0), B-doped (B/Ti = 0.03, Ta/Ti = 0), and Ta-doped TiO_2 (B/Ti = 0, Ta/Ti = 0.03) TiO_2 samples.

2.2. Material characterization

Powder X-ray diffraction patterns were recorded using a Bruker D2 Phaser diffractometer with a Cu Kα radiation source (λ = 1.54056 Å). The scan was recorded from 20 °C to 70 °C in 2θ, with a step size of 0.01 °C. Raman spectroscopy was performed on a Renishaw inVia Reflex micro-Raman spectrometer in the back-scattering geometry. The samples were excited by a 532 nm DPSS laser through a 50× objective lens, and the laser power was adjusted by NDF filters. X-ray photoelectron spectroscopy (XPS) measurements were performed on a Thermo Scientific K-Alpha spectrometer with a monochromatic Al Kα X-ray source of 1486.6 eV. All the binding energies were calibrated to the C 1s photoelectron peak at 284.8 eV, which is likely from surface hydrocarbon contamination. The obtained spectra were resolved into Gaussian–Lorentizan components after background subtraction. EDX spectra were recording on a JEOL JSM-5600LV SEM. All UV–vis diffuse reflectance spectroscopy measurements were carried out on a Shimadzu UV3600 UV-Vis-NIR spectrometer, using $BaSO_4$ fine powder as the reference.

2.3. Evaluation of photocatalytic performance

The photocatalytic activity of pure and doped TiO_2 was evaluated by monitoring the degradation of MB solution under simulated sunlight. 0.05 g as-prepared photocatalysts were dispersed in 50 ml MB solution with an initial concentration of 10^{-5} M in a quartz reaction tube, which was then stirred in the dark for 30 min to reach adsorption–desorption equilibrium. A 450 W xenon lamp was used as the simulated solar light source, which was placed vertically in a double-wall jacketed quartz tube with cooling water circulated between the quartz walls. In addition, a big fan was installed near the lamp to circulate air flow and maintain a nearly uniform temperature distribution inside the reactor. 4 ml of suspension was withdrawn at fixed time interval, and centrifuged to remove the catalysts. The change of MB concentration was determined by monitoring the absorbance at 660 nm (772s UV–vis spectrophotometer, Shanghai Optical Instrument) using the Beer–Lamber law.

3. Results and discussion

Fig. 1 shows recorded powder X-ray diffraction patterns of pure and doped TiO_2 samples. For pure titania, all the observed diffraction peaks at 2θ = 25.39°, 37.02°, 37.87°, 38.63°, 48.13°, 53.99°, 55.15°, and 53.99° can be assigned to anatase phase of TiO_2 crystal (JCPDF 21-1272). The diffraction patterns of doped TiO_2 nanocrystals are similar to that of the undoped sample no secondary phase related to B_2O_3 or Ta_2O_5 was detected. This implies that tantalum and boron ions are either successfully incorporated into the framework of TiO_2 crystal or well dispersed on the surface. Moreover, compared to pure TiO_2, the diffraction peaks of the doped samples shift toward smaller angle and the peak widths are increased (Table 1). The observed peak broadening indicates a smaller average crystallite size of doped samples. The average crystallite size

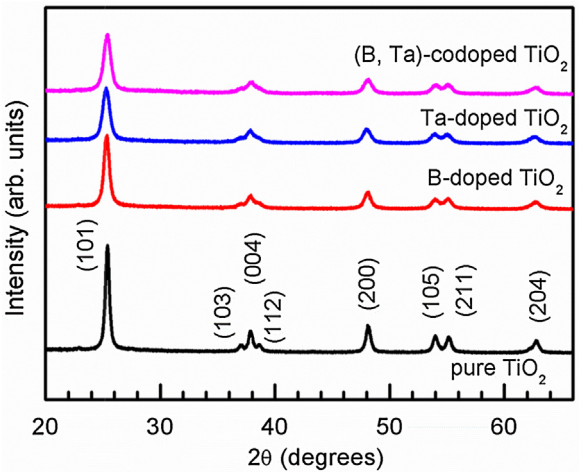

Fig. 1. X-ray diffraction patterns of pure, B and Ta singly doped, as well as (B, Ta)-codoped TiO_2 nanocrystals.